

Biomimetic Control of Mobile Robots based on the Information Processing Model of *Paramecium*

Akira Hirano[†], Toshio Tsuji[†], Noboru Takiguchi^{††}, and Hisao Otake^{†††}

[†]Graduate School of Engineering, Hiroshima Univ., Hiroshima 739-8527, Japan

^{††}Graduate School of Advanced Sciences of Matter, Hiroshima Univ., Hiroshima 739-8530, Japan

^{†††}Graduate School of Engineering, Osaka Univ., Osaka 565-0871, Japan

Abstract

In order to survive in complex natural environments, living organisms have been genetically acquiring various algorithms. Protozoans, for example, respond to various stimuli to search for a hospitable environment. Recently, the concept of *Software Biology* has been proposed, in which the algorithms of living organisms are considered as a kind of software that could be utilized for robot control.

Thus far, we have focused on the information processing algorithm of *Paramecium*, and proposed its computer model, *Virtual Paramecium*, based on biological knowledge. *Virtual Paramecium* can approximately realize the chemotactic behavior of the actual *Paramecium* based on the information processing model. In this paper, we report the results obtained when a mobile robot is controlled using *Virtual Paramecium*, and confirm the effectiveness of the biomimetic control based on the information processing algorithm of living organisms.

1 Introduction

In order to survive in complex natural environments, the genome of living organisms undergoes various changes, thereby forming various algorithms for survival. Recently, the concept of *Software Biology* has been proposed; this concept proposes the use of algorithms of living organisms for control of machines, that can adapt to environmental changes [1]. In the research field of adaptive control, neural networks have been introduced to control robots, and their effects have already been demonstrated. However, there is a possibility that the mechanism occurring in an actual living organism is not reflected in robot control because the cellular characteristics that comprise the neural network are very simple in comparison with a living cell. Hence, developing a computational model

of unicellular organism is considered one of the effective approach for achieving robot control.

Some models that focus on the internal processing system of living organisms have been proposed. The model called E-CELL [4] has been developed by Tomita et al. to simulate the behavior of the entire cell based on the chemical reaction, and another model has been developed by Bray and Lay [2] and Hauri and Ross [3] to simulate part of the internal processing of *E. coli* bacteria. Our research group has also developed the *E. coli* model based on the chemical equation of the internal processing system, and has applied it to mobile robot control [5, 6, 7].

At present, we are constructing a computational model of *Paramecium* [8, 9], *Virtual Paramecium*, because its internal processing system is more advanced than that of *E. coli*. Further, we have confirmed that *Virtual Paramecium* can reproduce the chemotactic response of a living *Paramecium* [9]. In this paper, we report the results of our study on the control of a mobile robot by using *Virtual Paramecium*; in addition, we confirm the effectiveness of the biomimetic control that is based on the information-processing algorithm of living organisms.

2 Paramecium

Paramecium can be assumed to be a discoid shape measuring approximately 250 μm in length and 50 μm in width; it has a uniform cilia layer on the cell surface. The direction of ciliary beat is modified by the stimuli from the environment. For instance, *Paramecium* accelerates their motion toward areas of low K⁺ concentration by increasing their ciliary beat frequency. On the other hand, *Paramecium* exhibits an escape reaction from areas of high K⁺ concentration, thereby accumulating in the areas of low K⁺ concentration. This response behavior with regard to the chemical environment is called chemotaxis.

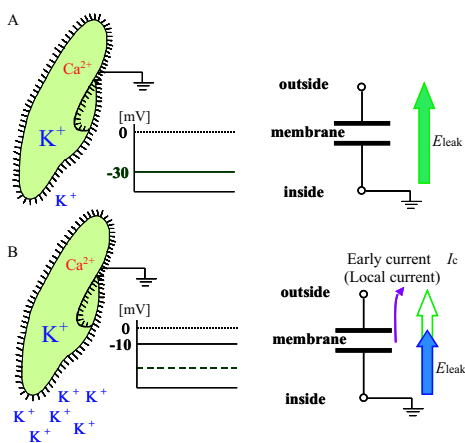


Figure 1: Membrane potential change of *Paramecium*.

Paramecium processes information by electrophysiological phenomena. Ion channels and ion pumps reside in the membrane, these proteins play an important role in maintaining the ionic connection between the interior and the exterior of the cell. In the cell, the Ca^{2+} concentration is maintained at a level lower than that of the external environment, while the K^+ concentration is maintained at a higher level. In a standard salt solution, the membrane potential is maintained at approximately 30 mV lower than that of the external environment when *Paramecium* does not receive the stimuli from the environment. When *Paramecium* receives a stimulus, the ion channels open and ionic flow occurs between the interior and the exterior of the cell. The membrane potential is then depolarized or hyperpolarized by the ionic flow. We consider that the depolarization of membrane potential occurs when *Paramecium* senses danger in the new environment; on the other hand, the hyperpolarization of membrane potential can be considered to occur when *Paramecium* senses that the new environment is safe. The ciliary movement is determined based on the information processed by the cell.

3 Virtual Paramecium

Virtual Paramecium comprises three units, namely, the sensory unit, information processing unit, and motor control unit. In this section, we describe the overview of each unit.

3.1 Sensory unit [9]

Figure 1 illustrates the relationship between the change in membrane potential and environmental

changes. It can be considered that a compulsory electrical change in membrane potential, similar to that in the voltage-clamp experiments [10], is generated when the ionic composition of the environment changes (see Figure 1). For instance, the resting membrane potential rises when the K^+ concentration in the environment increases, and then the potential difference generated between the environment and the interior of the cell decreases (see Fig. 1 A → B). An early current is generated as shown in Fig. 1B, when the cell of *Paramecium* is considered as a capacitor. Then, the sensory unit determines the probability of the aperture rate of ion channels that are opened by changed in the environmental conditions.

First, in the sensory unit, the resting membrane potential E_{leak} , which depends on $[\text{Ca}^{2+}]_o$ and $[\text{K}^+]_o$, is calculated by using the Goldman-Hodgkin-Katz equation [10]:

$$E_{\text{leak}} = \frac{\alpha_{\text{Ca}} E_{\text{Ca}} + \alpha_{\text{K}} E_{\text{K}}}{\alpha_{\text{Ca}} + \alpha_{\text{K}}}, \quad (1)$$

where α_{Ca} and α_{K} are the existence ratios of the Ca^{2+} and K^+ channels, respectively. Also, E_{Ca} and E_{K} are the equilibrium potentials which are generated by the difference in the concentration of ions inside and outside the cell. These are calculated using the following equation:

$$E_{\text{ion}} = \frac{RT}{cF} \ln \frac{[\text{ion}]_o}{[\text{ion}]_i} \quad (\text{ion} \in \{\text{Ca}^{2+}, \text{K}^+\}), \quad (2)$$

where c is the ionic valency, F the Faraday constant, R the gas constant, and T the absolute temperature. Also, $[\text{ion}]_o$ is the ionic concentration of the environment, and $[\text{ion}]_i$ the intracellular ionic concentration.

Then, the early current $I_c(t)$ is calculated by:

$$I_c(t) = \frac{1}{R_m} (E_{\text{leak}}(t) - V(t)), \quad (3)$$

where R_m is the input resistance of the membrane in *Paramecium*, and $V(t)$ the membrane potential. A positive value of $I_c(t)$ means outflow of current. In this study, it is assumed that the early aperture rate of each ion channel is proportional to the size of $I_c(t)$. The early aperture ratios of the Ca^{2+} channel and the K^+ channel are calculated as follows:

$$O_{\text{Ca}} = \begin{cases} b_{\text{Ca}} I_c & (I_c \geq \text{Th}_1) \\ 0 & (I_c < \text{Th}_1), \end{cases} \quad (4)$$

$$O_{\text{K}} = \begin{cases} 0 & (I_c > \text{Th}_2) \\ -b_{\text{K}} I_c & (I_c \leq \text{Th}_2), \end{cases} \quad (5)$$

where b_{Ca} , b_{K} , Th_1 , and Th_2 are constants. The early aperture rate O_{Ca} of the Ca^{2+} channel increases when

the early current is larger than the threshold Th_1 and flows outwards ($I_c \geq Th_1 > 0$). Conversely, the early aperture rate O_K of the K^+ channel increases when the early current is smaller than the threshold Th_2 and flows inwards ($I_c \leq Th_2 < 0$). Thus, the early aperture rate of each ion channel is determined corresponding to the change in the environmental conditions.

3.2 Infomation processing unit [8]

In this unit, the change in membrane potential and the Ca^{2+} concentration in cilia are calculated using the inputs of the sensory unit.

First, the changes in the membrane potential of *Paramecium* are modeled as follows:

$$\dot{V}(t) = \frac{1}{C_m} [I_c(t) - I_{Ca}(t, V) - I_K(t, V) - I_{leak}(t, V)], \quad (6)$$

where $V(t)$ is the membrane potential, $I_c(t)$ is the early current, and C_m is the membrane capacity. The Ca^{2+} current $I_{Ca}(t, V)$, the K^+ current $I_K(t, V)$, and the leakage current $I_{leak}(t, V)$ are given by the following equations [8]:

$$I_{Ca}(t, V) = \bar{g}_{Ca} m^5 \{1 - (1 - h)^5\} (V(t) - E_{Ca}), \quad (7)$$

$$I_K(t, V) = \bar{g}_K n (V(t) - E_K), \quad (8)$$

$$I_{leak}(t, V) = g_{leak} (V(t) - E_{leak}), \quad (9)$$

where \bar{g}_{Ca} , \bar{g}_K , and g_{leak} are the maximum values of the ion conductance for Ca^{2+} , K^+ , and leakage ion channels, respectively. Equilibrium potentials for Ca^{2+} , K^+ , and leakage ions are expressed as E_{Ca} , E_K , and E_{leak} , respectively. Also, m , h , and n are the activation probabilities of each ion channel. Activation probabilities, $x \in \{m, h, n\}$, of each channel are calculated based on the Hodgkin-Huxley equations [11] as follows:

$$\begin{aligned} \dot{m}(t, V, O_{Ca}) &= \alpha_m(V, O_{Ca}) \cdot (1 - m(t, V, O_{Ca})) \\ &\quad - \beta_m(V) \cdot m(t, V, O_{Ca}), \end{aligned} \quad (10)$$

$$\begin{aligned} \dot{h}(t, V, O_{Ca}) &= \alpha_h(V, O_{Ca}) \cdot (1 - h(t, V, O_{Ca})) \\ &\quad - \beta_h(V) \cdot h(t, V, O_{Ca}), \end{aligned} \quad (11)$$

$$\begin{aligned} \dot{n}(t, V, O_K) &= \alpha_n(V, O_K) \cdot (1 - n(t, V, O_K)) \\ &\quad - \beta_n(V) \cdot n(t, V, O_K). \end{aligned} \quad (12)$$

O_{Ca} and O_K are the early open ratios of the Ca^{2+} channel and the K^+ channel that are calculated by the sensory unit. The complicated changes in depolarization are realized by the above mechanism.

Next, the Ca^{2+} concentration in cilia is calculated. Deciliated *Paramecium* whose cilia are removed by

chemical treatment is utilized in order to formulate the electrical characteristics of only the cell body. The changes in the membrane potential are given as:

$$\begin{aligned} \dot{V}(t) &= \frac{1}{C_m} [I_c(t) - I_{Ca(cell)}(t, V) \\ &\quad - I_K(t, V) - I_{leak}(t, V)], \end{aligned} \quad (13)$$

where $I_{Ca(cell)}$ is the current in the cell of the deciliated *Paramecium*, and is defined by the following equation:

$$\begin{aligned} I_{Ca(cell)} &= \bar{g}_{Ca(cell)} m_{(cell)}^5 \{1 - (1 - h_{(cell)})^5\} \\ &\quad (V(t) - E_{Ca}), \end{aligned} \quad (14)$$

where $\bar{g}_{Ca(cell)}$ is the maximum value of the ion conductance for the Ca^{2+} channel in the cell, and $x_{(cell)}$ ($x \in \{m, h\}$) is the activation probability in only the cell body defined by:

$$\begin{aligned} \dot{x}_{(cell)}(t, V, O_{Ca}) &= \alpha_{x_{(cell)}}(V, O_{Ca}) \\ &\quad \cdot (1 - x_{(cell)}(t, V, O_{Ca})) \\ &\quad - \beta_{x_{(cell)}}(V) \cdot x_{(cell)}(t, V, O_{Ca}). \end{aligned} \quad (15)$$

By using both $I_{Ca(cell)}$ and the Ca^{2+} current I_{Ca} in the whole *Paramecium*, the Ca^{2+} current in cilia $I_{Ca(cilia)}$ is expressed as:

$$I_{Ca(cilia)} = I_{Ca} - I_{Ca(cell)}. \quad (16)$$

Thus, the ionic flow of Ca^{2+} in the cell body and that in cilia can be separated. Finally, the Ca^{2+} concentration in cilia is calculated as follows :

$$\frac{d [\text{Ca}^{2+}]_{in}}{dt} = -\frac{1}{2F} [I_{Ca(cilia)} + (I_p)_{Ca}], \quad (17)$$

$$(I_p)_{Ca} = 2F \frac{(\bar{J}_p)_{Ca}}{1 + \left(\frac{K_m}{[\text{Ca}^{2+}]_{in}}\right)^3}, \quad (18)$$

where $[\text{Ca}^{2+}]_{in}$ is the Ca^{2+} concentration in cilia, F the Faraday constant, $(\bar{J}_p)_{Ca}$ the maximum active Ca^{2+} extrusion, and K_m the $[\text{Ca}^{2+}]_{in}$ at which the active Ca^{2+} extrusion is at half its maximum value. Also, $(I_p)_{Ca}$ is the current produced by the Ca^{2+} pump which discharges Ca^{2+} to the exterior of the cell, and it is assumed that $(I_p)_{Ca}$ is included in I_{leak} calculated by Eqs. (6) and (13) for simplicity.

3.3 Motor control unit

During its movements through water, *Paramecium* follows a spiral path while rotating around its long axis [12]. This is one of the effective mechanisms that can be employed to escape from the dangerous elements in an environment. The proposed *Virtual Paramecium*

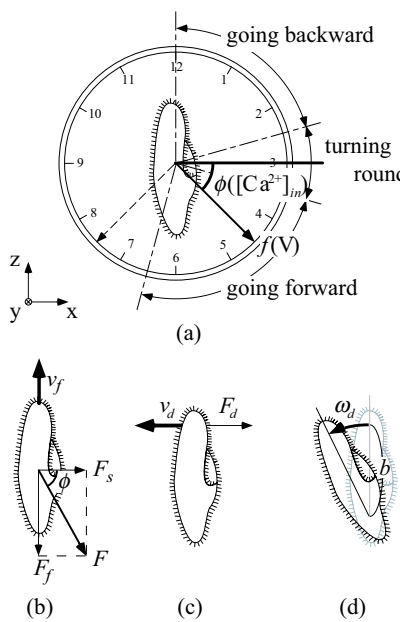


Figure 2: Driving forces generated by ciliary movements.

[9] reproduces the behavior of an actual *Paramecium*. Here, we describe the motor control unit and the planar movements of *Virtual Paramecium* in order to apply it to control of mobile robots.

The swimming condition of *Paramecium* depends on the frequency and direction of the ciliary beat. It is easy to understand the direction of the ciliary beat of *Paramecium* by considering the front of *Paramecium* as the direction corresponding to 12 o'clock on an analog clock, as shown in Figure 2(a) [10]. As *Paramecium* senses stimuli, the direction of the ciliary beat changes between half past six and 12 o'clock, while it is half past four in the normal condition (see Figure 2(a)). The swimming velocity increases when the ciliary beat direction approaches 6 o'clock. Also, *Paramecium* moves backward as the ciliary beat direction approaches 12 o'clock. The driving force F can be resolved into the driving power F_d and the rotational power F_s (see Figure 2(b)). In addition, it is possible to determine the spiral movement in combination with F_d , which is generated by the movement of peculiar cilia around the peristome [12].

The ciliary beat direction is regulated by the Ca^{2+} concentration in cilia [10, 13]. First, the ciliary beat direction $\phi([\text{Ca}^{2+}]_{in})$ is modeled as the following functions of $[\text{Ca}^{2+}]_{in}$:

$$\phi([\text{Ca}^{2+}]_{in}) = \pi \left(\frac{1}{A_\phi \log_{10}([\text{Ca}^{2+}]_{in})} - 0.5 \right)$$

$$\begin{aligned} (A_\phi = A_{\phi 1} & \quad ([\text{Ca}^{2+}]_{in} < C_\phi)) \\ (A_\phi = A_{\phi 2} & \quad ([\text{Ca}^{2+}]_{in} \geq C_\phi)), \end{aligned} \quad (19)$$

where $A_{\phi 1}$ and $A_{\phi 2}$ are constants that determine the direction of the ciliary beat, and C_ϕ is the concentration value of $[\text{Ca}^{2+}]_{in}$ when the direction of the ciliary beat approaches 3 o'clock.

The ciliary beat frequency is regulated by the membrane potential [14]. Although the steady-state frequency of the ciliary beat is 10 – 20 Hz, it is increased to approximately 50 Hz corresponding to the change in the membrane potential. In addition, the ciliary beat frequency decreases when the Ca^{2+} concentration increases to more than $10^2 \mu\text{M}$. Therefore, the ciliary beat frequency, $f(V, [\text{Ca}^{2+}]_{in})$, is modeled as the following equations of the membrane potential:

$$f(V, [\text{Ca}^{2+}]_{in}) = f(V) - f([\text{Ca}^{2+}]_{in}), \quad (20)$$

$$f(V) = f_0 + A_{f1}(|A_{freq} - V(t)|)^{A_{f2}}, \quad (21)$$

$$f([\text{Ca}^{2+}]_{in}) = \left(\frac{f_{max}}{1 + \exp(A_{f3} \log_{10}(A_{f4} [\text{Ca}^{2+}]_{in}))} \right), \quad (22)$$

where A_{fi} ($i = 1, 2, 3, 4$) are constants, f_0 the steady-state value of ciliary beat frequency, f_{max} the maximal value, and A_{freq} the membrane potential value during the resting beat frequency. The driving force F is calculated as follows:

$$F = a_0 f(V, [\text{Ca}^{2+}]_{in}), \quad (23)$$

where a_0 is the coefficient which transforms the ciliary beat frequency into the driving force F in *Paramecium*.

By using Eqs. (19), (20), ..., (23), the movements of *Paramecium* in two-dimensional space can be calculated. The velocity of *Paramecium* is calculated by:

$$v_f = -a_1 F \sin(\phi), \quad (24)$$

where v_f is the velocity in the longitudinal direction of body, and a_1 is the coefficient which transforms the driving force into v_f (see Figure 2(b)). The velocity v_d , which is perpendicular to the longitudinal axis, and the turning angle velocity ω_d by v_d are given by the following equations:

$$v_d = -a_2 f_d, \quad (25)$$

$$\omega_d = \frac{v_d}{b}, \quad (26)$$

where a_2 is a coefficient that transforms f_d into v_d and b is the distance between the fulcrum of rotation and

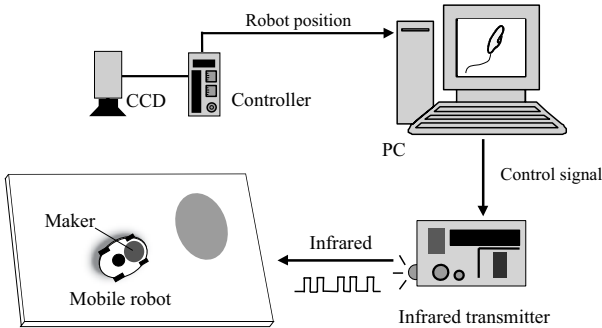


Figure 3: Mobile robot control system.

the point of application of f_d (see Figure 2(c), (d)). The orbital period of spiral movement in *Paramecium* is defined as T_f , and the sign of F_d is inverted from positive to negative, or vice versa, in every $T_f/2$ period. Thus, it is possible to reproduce the serpentine movement that the spiral movement of *Paramecium* is projected on the two-dimensional plane.

4 Biomimetic control experiments

4.1 Control system configuration

Figure 3 illustrates the control system for a mobile robot. The biomimetic control experiments of a mobile robot were carried out according to the following procedure. DQ-04 (TAKARA), whose length is approximately 5 cm, was adopted as the mobile robot. This robot has four wheels in the front and rear, and only two rear wheels on the right and left can be controlled independently. In these experiments, an image processing system was adopted for environmental measurement because it was difficult to mount any sensors on the robots. The measurement area was square (2.5 m × 2.5 m), and the two-dimensional position of a marker on the head of the robot was measured using a CCD camera suspended from the ceiling. The virtual chemical environment was set as a function of the position in the horizontal plane beforehand. The chemical concentration was input to the sensory unit of *Virtual Paramecium* every 40 millisecond. *Virtual Paramecium* processes the input information and determines the control input to the robot. Then, the control signal was sent to the robot to realize the comparable behavior to the actual organisms calculated by *Virtual Paramecium*.

4.2 Cruise control of the mobile robot

The relationship between the rotation speed of the two rear wheels in the mobile robot and its movement

can be given by the following equation:

$$\begin{bmatrix} v \\ \omega \end{bmatrix} = \begin{bmatrix} \frac{1}{2} & -\frac{1}{2} \\ \frac{1}{2c_r} & -\frac{1}{2c_r} \end{bmatrix} \begin{bmatrix} v_L \\ v_R \end{bmatrix}, \quad (27)$$

where $2c_r$ is the length of the axle; and v_L and v_R are the speeds of the rear wheels. In these experiments, each rear wheel was controlled according to the following equation:

$$\begin{bmatrix} v_L \\ v_R \end{bmatrix} = \gamma \begin{bmatrix} \frac{1}{2} & -\frac{1}{2} \\ \frac{1}{2c_r} & -\frac{1}{2c_r} \end{bmatrix}^{-1} \begin{bmatrix} v_f \\ \omega_d \end{bmatrix}, \quad (28)$$

where γ is a coefficient that transforms the movement velocity of *Virtual Paramecium* into the mobile robot, in consideration of each size. The values of v_f and ω_d are calculated using the motor control model (24) and (26).

4.3 Experimental results

The biomimetic control of a mobile robot was executed using *Virtual Paramecium*. The parameters included in *Virtual Paramecium* were determined based on previous studies [9, 10].

In this paper, reactions of the mobile robot toward the area where the K^+ concentration was different from that of the standard salt solution were examined. The results obtained when the K^+ concentrations of the stimulation solution were set to 16 mM and 0.25 mM are shown in Figure 4(a) and (b), respectively. The left side of Figure 4 shows the trajectories of the mobile robot, while the right side shows the time course of the swimming velocities of *Virtual Paramecium*, which the negative velocity implies backward movement.

Figure 4(a) shows the escape reaction of the mobile robot from the area where the K^+ concentration is higher than that of the standard salt solution. Further, the mobile robot exhibited accelerated movement toward the area where the K^+ concentration was lower than the standard salt solution (see Figure 4(b)). Additionally, in Figure 4(b), the escape reaction to the area of standard salt solution is shown after cruising in the environment with low K^+ concentration for a short duration. On the basis of above results, we confirmed the effectiveness of the biomimetic control that was based on the information processing algorithm of living organisms.

5 Summary

In this paper, the results of our study on the control of a mobile robot by using *Virtual Paramecium* have

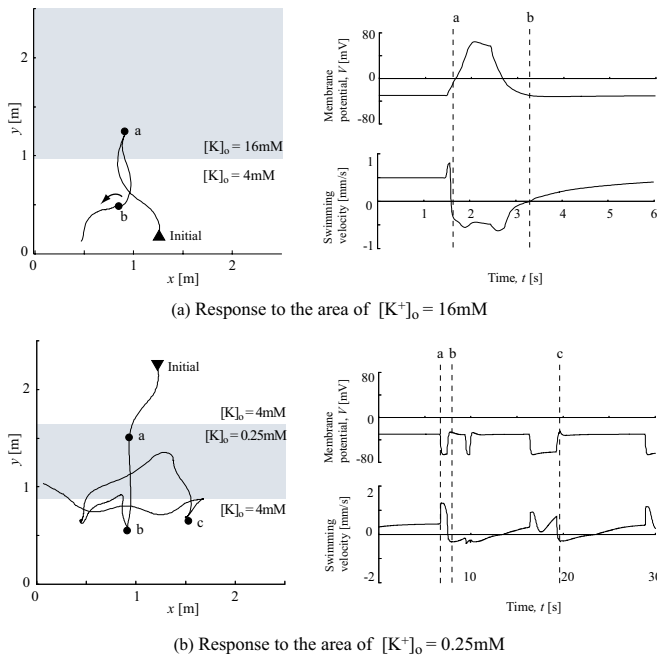


Figure 4: Responses of a mobile robot to the virtual chemical environments.

been reported. We confirmed that the escape reaction increased in the area where the K^+ concentration was higher than that of the standard salt solution, and the mobile robot attempts to continue to reside in the area with a low concentration of K^+ . On the basis of above results, we confirmed the effectiveness of the biomimetic control that was based on the information processing algorithm of living organisms.

In future research, our experimental results will be compared to the control results by using the information processing algorithm of *E. coli* bacteria [7].

Acknowledgements

This work is partially supported by the 21st Century COE Program of JSPS (Japan Society for the Promotion of Science) on *Hyper Human Technology toward the 21st Century Industrial Revolution*.

References

- [1] H. Otake (1998) : "Software of living organisms," KYORITSU SHUPPAN CO., LTD.. (in Japanese)
- [2] D.Bray, and S.Lay (1994) : "Computer Simulated Evolution of a Network of Cell-Signaling Molecules", *Biochemical Journal*, Vol. 66, pp. 972–977.
- [3] D. C. Hauri and J. Ross (1995) : "A Model of Excitation and Adaptation in Bacterial Chemotaxis", *Biochemical Journal*, Vol. 68, pp. 708–722.
- [4] M. Tomita, K. Hashimoto, K. Takahashi, T. S. Shimizu, Y. Matsuzaki, F. Miyoshi, K. Saito, S. Tanida, K. Yugi, J. C. Venter, C. A. Hutchison III (1999) : "E-CELL: software environment for whole-cell simulation," *Bioinformatics*, Vol. 15, No. 1, pp. 72–84.
- [5] T. Morohoshi, T. Tsuji, H. Otake (1998) : "A Model of Bacterial Motor Control and Computer Simulation of the Chemotaxis," *Journal of the Society of Instrument and Control Engineers*, Vol. 34, No. 11, pp. 1731–1738. (in Japanese)
- [6] T. Tsuji, K. Hashigami, M Kaneko, H. Otake (2002) : "Emerging chemotaxis of virtual bacteria using genetic algorithm," *Transaction of IEE of Japan*, Vol. 122-C, pp. 201–207. (in Japanese)
- [7] T. Tsuji, A. Sakane, O. Fukuda, M. Kaneko, H. Otake (2002) : "Bio-mimetic control of mobile robots based on a model of bacterial chemotaxis", *Trans. of the Japan Society of Mechanical Engineers*, Vol. 68, No. 673, pp. 171–178. (in Japanese)
- [8] A. Hirano, T. Tsuji, N. Takiguchi, H. Otake (2005) : "Modeling of the Membrane Potential Change of *Paramecium* for Mechanical Stimuli", *SICE Symposium on Decentralized Autonomous Systems*, Vol. 41, No. 4, pp.351–357. (in Japanese)
- [9] A. Hirano (2005) : "A Model of Chemotactic Response of Paramecium Based on Electrophysiology," Dissertation for the degree of Master of Engineering, Graduate School of Engineering, Hiroshima University.
- [10] Y. Naitoh (1990) : "Behavior of unicellular animals," University of Tokyo Press. (in Japanese)
- [11] A.L.Hodgkin and A.F.Huxley (1952) : "A Quantitative Description of Current and Its Application to Conduction and Excitation in Nerve," *The Journal of Physiology*, Vol. 117, pp. 500–544.
- [12] K. Sugino and Y. Naitoh (1988) : "The method for measuring a helical trajectory of Paramecium," *Medical science*, Igaku-Shoin Ltd., Vol. 39, No. 5, pp.485–490. (in Japanese)
- [13] Y. Naitoh and H. Kaneko (1972) : "Reactivated Triton-Extracted Models of Paramecium: Modification of Ciliary Movement by Calcium Ions," *Science*, Vol. 176, pp. 523–524.
- [14] P. Brehm and R. Echkert (1978) : "AN ELECTROPHYSIOLOGICAL STUDY OF THE REGULATION OF CILIARY BEATING FREQUENCY IN *PARAMECIUM*," *J. Physiol.*, 283, pp. 557–568.